

Unexpected observations of the heavy-ion fusion excitation function above the Coulomb barrier

Nate Watwood^{1,*}, Cheng Lie Jiang^{1,**}, Walter Henning¹, Calem Hoffman¹, and Ben Kay¹

¹Physics Division, Argonne National Laboratory, Argonne, Illinois 60439, USA

Abstract. Two unexpected behaviors have been observed in heavy-ion fusion excitation functions at energies above the Coulomb barrier. The first behavior is observed in overlapping excitation spectra. Fusion excitation functions $\sigma(E)$ that have different entrance channels but fuse to the same compound nucleus appear to overlap in the energy domain above the barrier. The overlap emerges after scaling the center of mass energy of each excitation function by a constant scaling factor, SF. The second behaviour stems from the structure of the fusion excitation curve. Contrary to descriptions from coupled-channels or other model calculations, heavy-ion fusion excitation functions are not smooth near and above the Coulomb barrier. There appears to be weak but noticeable oscillations or structures within the excitation functions that can be observed clearly in the representation $d(\sigma E)/dE$ and in comparison with theoretical calculations $\sigma(E) - \sigma_{th}(E)$. Moreover, the corresponding $d(\sigma E)/dE$ spectra for systems that form the same compound nucleus also overlap well in this energy range, including their fine structures, but the uncertainty is large. It appears the two behaviors are correlated and the reasoning behind these behaviors are yet unknown, but may be due to the compound-channel effect.

1 Introduction

The study of heavy-ion fusion began in earnest in the 1970's from an interest in expanding the periodic table beyond what was possible with neutrons and light-charged particles. Since then the data for over a thousand heavy-ion fusion excitation functions has been accumulated, with cross sections ranging nine orders of magnitude, from barns to nanobarns. The data from these experiments led to the discovery and study of several behaviors in the fusion excitation function, including sub-barrier fusion enhancement, deep sub-barrier hindrance, and the barrier distribution and its effect on reaction dynamics. These behaviors are the result of the nuclear structure of the colliding nuclei and compound nucleus as well as various aspects of nuclear reaction dynamics. Most of these behaviors have been discussed in depth in review articles [1–6].

Two behaviors of the heavy-ion fusion excitation function will be discussed in this proceedings, which were observed from the systematic reanalysis of previously measured fusion reaction data [7, 8]. The first is the direct influence of the compound nucleus on heavy-ion fusion excitation functions, or the compound channel effect, and the second is an oscillation phenomenon of the fusion excitation function at energies above the barrier.

2 Compound Channel Effect

The fusion excitation function is shaped primarily by the entrance channel, the character of the two colliding nuclei,

and the compound channel effect, the resulting compound nucleus. Present knowledge of fusion cross sections generally rely on the entrance channel, e.g. coupled-channels (CC) calculations, where the direct influences of the compound channel aren't obviously displayed. In these calculations, the compound channel effects are simulated by an adjustment of the parameters from the entrance channels. Even in the quantum mechanical equation for the fusion cross section as a function of center-of-mass energy $\sigma(E) = \frac{\pi}{k^2} \sum_l (2l+1) T_l(E)$, which is a direct counting of each entrance channel with wavelength k , angular momentum l , and quantum mechanical coefficient $T_l(E)$, the nature of the compound nucleus likely hides implicitly. A re-evaluation of available experimental data has presented new insights and may exhibit evidence of the compound channel effect.

In a previous study of entrance-channel effects, the fusion excitation functions of three fusion reactions, $^{19}\text{F} + ^{197}\text{Au}$, $^{12}\text{C} + ^{204}\text{Pb}$, and $^{30}\text{Si} + ^{180}\text{W}$ were measured [9, 10], and all three reactions formed the same compound nucleus, ^{216}Ra . The fusion cross sections consisted of the sum of the evaporation residue cross sections and the fusion fission cross sections, measured separately. The results of the study are shown in Fig 1(a), where the fusion cross sections are a function of center-of-mass energy (solid) and compound nucleus excitation energy (open). While qualitatively these curves look similar, it is difficult to make a direct comparison due to their differing Coulomb interactions.

There are common reduction methods to compare fusion excitation functions for different systems [11, 12]. Since the influence of channel couplings at above-barrier

*e-mail: nwatwood@anl.gov

**e-mail: cjiang@anl.gov

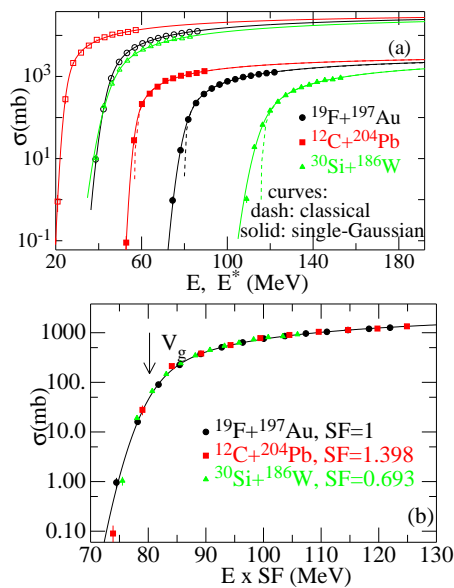


Figure 1. (a) The fusion excitation functions for three reactions that lead to the same compound nucleus ^{216}Ra . Solid points are for cross sections as a function of center-of-mass energy, E , and open symbols as a function of compound nucleus excitation energy E^* (scaled by a factor 10). Solid curves are the results of a least-squares fit from the single-Gaussian model, and dashed curves are predictions from the classical model. (b) Scaled fusion excitation functions for the same three reactions, where the energies are multiplied by a scaling factor (SF).

energies is negligible, the barrier heights and radii can be extracted from above-barrier fusion data and can then be used in different reduction procedures to compare different systems. An investigation of these reduction methods for fusion found some to be reliable at above and below energies [11]. A drawback of using these reduction methods is that the cross sections are reduced by the interaction radius and some of the physical quantity becomes lost. In this work, a new method is introduced that removes the influence of the Coulomb interaction while preserving the physical quantity of the cross section. In this method, the fusion center-of-mass energies of the compared systems are multiplied by a scaling factor (SF) such that all fusion excitation functions overlap. In practice, one of the reactions is set to SF=1 for one reaction, and the others are adjusted accordingly to achieve maximum overlap. This proposed representation, the *scaled fusion excitation function*, can be seen in Fig 1(b), where the scaling factors are SF=1.000, 1.413, and 0.693 for the $^{19}\text{F} + ^{197}\text{Au}$, $^{12}\text{C} + ^{204}\text{Pb}$, and $^{30}\text{Si} + ^{186}\text{W}$ reactions, respectively.

The single-Gaussian barrier distribution model was used to extract the parameters from the data, V_g , R_g , and W_g , the barrier height, interaction radius, and standard deviation of the distribution, respectively. This model has been shown to reproduce the fusion excitation function well across a large energy domain [13–17]. The cross section for this model is represented as

$$\sigma_g(E) = \frac{\sqrt{\pi}R_g^2W_g}{\sqrt{2}E} [\sqrt{\pi}Zerfc(-Z) + \exp(-Z^2)] \quad (1)$$

where $Z = (E - V_g)/\sqrt{2}W_g$, and the barrier distribution is

$$D_g(B) = \frac{1}{\sqrt{2\pi}W_g} \exp\left[-\left(\frac{B - V_g}{\sqrt{2}W_g}\right)^2\right]. \quad (2)$$

A least-squares fit of Equation 1 was applied to the excitation functions and are represented as solid curves in Figure 1, where they reproduce the data well. Also shown is the classical model, represented by dashed curves, and follows the equation

$$\sigma(E)E = \pi R^2(E - V_c), \quad (3)$$

where R is the interaction radius and V_c is the barrier height. The parameters extracted from the single-Gaussian method are shown in Table 1 from the publication of Jiang *et al.* [8] in comparison with the Coulomb barrier V_0 and barrier radius R_0 determined from the Winther model [18] as well as the ratios of the classical barrier values to the values from the two different models, represented as r_g and r_w .

Figure 1(b) shows the scaled excitation functions of the three systems all leading to the same compound nucleus ^{216}Ra , with the Coulomb barrier of the $^{19}\text{F} + ^{197}\text{Au}$ reaction (SF=1) indicated by V_g . The overlap between the excitation functions is quite good, with the exception of one data point from the $^{12}\text{C} + ^{204}\text{Pb}$ reaction around 0.1 mb.

Three additional comparisons using the scaled excitation function are shown in Figure 2: $^{28}\text{Si} + ^{142}\text{Ce}$, $^{32}\text{S} + ^{138}\text{Ba}$, $^{48}\text{Ti} + ^{122}\text{Sn}$ forming the compound nucleus ^{170}Hf [19]; $^{30}\text{Si} + ^{170}\text{Er}$ and $^{19}\text{F} + ^{181}\text{Ta}$ forming the compound nucleus ^{200}Pb [20]; $^{31}\text{P} + ^{175,176}\text{Lu}$ and $^{28,29}\text{Si} + ^{178}\text{Hf}$ forming the compound nucleus $^{206,207}\text{Rn}$ [21]. It is clear from these figures that, using the scaling excitation function method, all systems forming the same compound nucleus overlap in the energy domain above the barrier.

All of the data presented in the figures thus far were measured by the same authors with the same experimental setup, reducing the systematic uncertainty. While this is useful for the comparisons presented here, it is much more likely that fusion data are measured in different facilities with different setups. For instance, $^{58}\text{Ni} + ^{64}\text{Ni}$ and $^{32}\text{S} + ^{90}\text{Zr}$ forming the compound nucleus ^{122}Ba [22, 23], $^{64}\text{Ni} + ^{64}\text{Ni}$, $^{32}\text{S} + ^{96}\text{Zr}$, $^{28}\text{Si} + ^{100}\text{Mo}$, and $^{16}\text{O} + ^{112}\text{Cd}$ forming the compound nucleus ^{128}Ba [23–26], and $^{28}\text{Si} + ^{64}\text{Ni}$ and $^{30}\text{Si} + ^{62}\text{Ni}$ forming the compound nucleus ^{92}Mo [27, 28], all were measured at different facilities. The scaled excitation function method was applied to these data and the extracted parameters are shown in Table 1 from the publication of Jiang *et al.* [8]. While they are not overwhelmingly conclusive, there does not seem to be disagreement to the proposed overlap observations.

To determine whether this overlap phenomenon as a result of the scaled excitation function method is exclusive to reactions forming the same compound nucleus, a

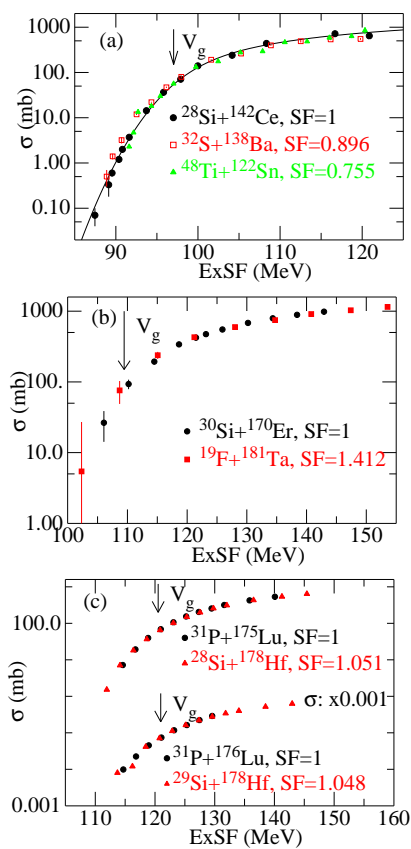


Figure 2. Scaled fusion excitation functions for reactions that form the compound nucleus ^{170}Hf (a) ^{200}Pb (b) and $^{206,207}\text{Rn}$ (c), each with their respective scaling factor.

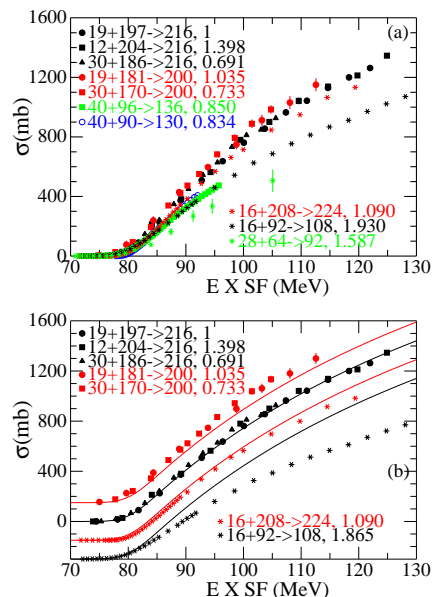


Figure 3. (a) Comparison of scaled excitation functions. Reactions that form the same compound nucleus are color coded. (b) Comparison of scaled excitation functions for reactions that form the same compound nucleus (scaled by 150 mb per differing compound nucleus) to the single-Gaussian model fit of $^{19}\text{F}+^{197}\text{Au}$ (solid lines).

comparison to reactions forming different compound nuclei must be made. Figure 3(a) shows such a comparison for compound nuclei of mass $A=108, 130, 136, 200, 216$, and 224, where each fusion excitation function is color coded to the compound nucleus it forms.

While some of the differences are quite small, it is clear that the shape of the fusion excitation function is dependent on the compound nucleus formed. To illustrate the differences more clearly, several fusion excitation functions from Figure 3(a) are shown again in Figure 3(b), where reactions that form different compound nuclei are separated by 150 mb. The single-Gaussian model fit for $^{19}\text{F}+^{197}\text{Au}$, forming compound nucleus ^{216}Rn , is imposed over each excitation function as a solid curve and serves as a reference to guide the eye. Looking at each of these comparisons, it is clear there is a difference in shape of the scaled excitation function for reactions that form different compound nuclei. In general, there seem to be larger differences in scaled excitation function shape with increasing difference in compound nucleus mass, but it is not exact, and other factors should contribute as well.

This observation that each compound nucleus has a distinct universal shape of the reduced excitation function leads to the possibility of extracting information about the compound-channel effect, which may be excluded from descriptions of the fusion excitation function based on the classical or incoming wave boundary condition approximations.

3 Oscillations or Resonance Phenomenon

The fusion excitation function, in a simplistic view, is produced by the Coulomb barrier between the two colliding nuclei and is expected to continuously increase from low to high bombarding energy. The structure of the excitation function, whether it is monotonic or more complex, has been a subject of interest. The first observation of complex structure was in the 1960's with the $^{12}\text{C} + ^{12}\text{C}$ reaction [29], first with elastic scattering and then for various other reactions, including fusion. Since then this structure phenomenon has been well studied and outlined in a set of Treatises by Bromley [30]. More recently, structures in the excitation functions of $^{20}\text{Ne} + ^{20}\text{Ne}$ and $^{28}\text{Si} + ^{28}\text{Si}$ observed and discussed by Poffe [31] and Esbensen [32]. The explanation in these cases was that the reactions were symmetric and only incident waves with even angular momentum could contribute, yielding relatively large separations in energy between successive angular momentum barriers. Esbensen showed good agreement between CC calculations and the fusion cross sections for these reactions.

The most common representation of the excitation function, $\sigma(E)$, is in either linear or log scale as a function of center-of-mass energy. This gives the general shape of the excitation over a broad energy range, but it is often difficult to discern more subtle structures or deviations from theoretical predictions. Other representations have thus been used to highlight these fluctuations, each emphasizing the detailed behavior of the excitation function for a specific energy range [6].

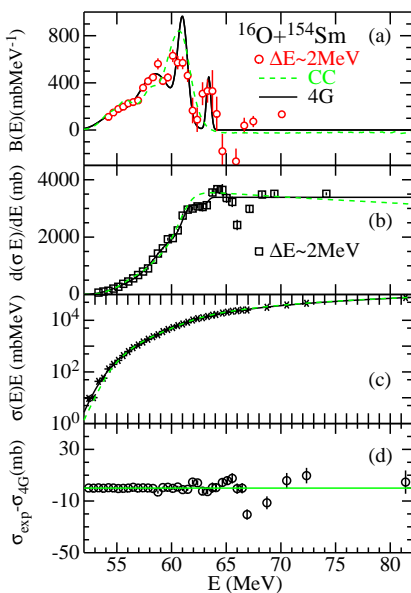


Figure 4. Various representations of the fusion excitation function for the $^{16}\text{O} + ^{154}\text{Sm}$ reaction compared to CC calculations (green curve) and the four-Gaussian model fit (black curve).

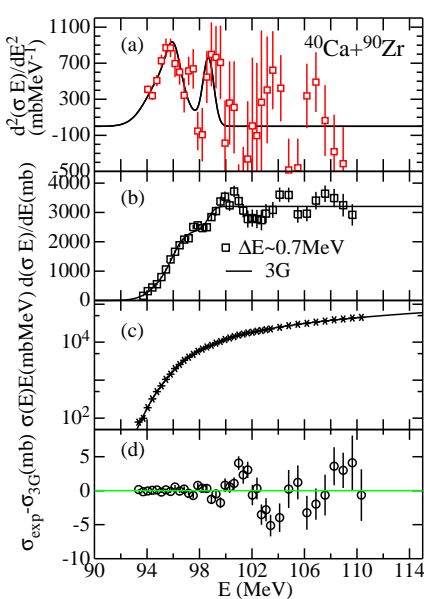


Figure 5. Various representations of the fusion excitation function for the $^{40}\text{Ca} + ^{90}\text{Zr}$ reaction compared to the three-Gaussian model fit (black curve).

One example is the second derivative of the energy cross section $d^2(\sigma(E))/dE^2$, introduced by Rowley et al. [33], which was used to show evidence of structure in the fusion excitation function near the fusion barrier. Under the classical approximation, this structure, or barrier distribution, could be obtained and reproduced by different channels coupling effects in coupled channels (CC) calculations.

It has been recently shown that barrier distributions of heavy-ion fusion excitation functions can be well described by fitting a three- or four-Gaussian spectrum [14, 17]. The resulting cross section curve obtained from this fit is an analytic function that reproduces the excitation function well, sometimes even better than CC calculations.

Using the multiple representations of fusion cross section and the multi-Gaussian fit method, a re-evaluation of available data shows evidence of an oscillation phenomenon at energies above the barrier that may be attributed to resonance phenomenon and cannot be reproduced by CC calculations.

Four representations of the fusion cross section, σE , $d(\sigma E)/dE$, $d^2(\sigma E)/dE^2$, and $\sigma_{exp} - \sigma_G$ are shown in Figure 4 for the reaction $^{16}\text{O} + ^{154}\text{Sm}$ [35] and are compared to the Gaussian barrier distribution method and CC calculations. The data in panels (a) and (b) are deduced from previous results and are calculated from the single- and double- differentiation methods, with ΔE representing the energy steps used.

A comparison of CC calculations and the Gaussian barrier distribution method in Figure 4(c) shows good agreement with the experimental data in the $\sigma(E)E$ representation across the full energy range, but as previously discussed, this representation does not show the more subtle structures within the excitation spectrum. The first and second derivative representations in Figure 4(a) and (b) be-

gin to highlight these structures. In these representations, CC calculations and the Gaussian distribution method reproduce the experimental data well at lower energies, but only give an average behavior at higher energies. That is to say, the experimental data displays oscillations or structures in the higher energy region not reproduced by either theoretical method. This phenomenon is highlighted even further in Figure 4(d), which shows the residuals of the experimental data and the four-Gaussian method.

Figure 5 shows the same representations for the $^{40}\text{Ca} + ^{90}\text{Zr}$ [36] reaction. In this data as well, while there is no indication of underlying structure in the $\sigma(E)E$ representation of the fusion cross section, oscillations or structures begin to appear at higher energies for the $d(\sigma E)/dE$, $d^2(\sigma E)/dE^2$, and $\sigma_{exp} - \sigma_G$ representations that cannot be reproduced by the multi-Gaussian method. The shape and amplitude of the oscillations are unique for both systems and seem to depend on the reaction. It must be noted that similar single- and double- differentiated spectra were shown in the original papers [34–36], but due to the large uncertainties and negative barrier values, a detailed study was not given to these behaviors.

A subsequent investigation found that this oscillation behavior is not unique to these two reactions, rather it seems to be common for heavy-ion fusion. Five more reactions, $^{16}\text{O} + ^{208}\text{Pb}$ [37], $^{34}\text{S} + ^{168}\text{W}$ [38], $^{40}\text{Ca} + ^{192}\text{Os}$ [39], $^{40}\text{Ca} + ^{94}\text{Zr}$ [36], and $^{40}\text{Ca} + ^{96}\text{Zr}$ [40] are shown in Figures 6 and 7 with the single-differentiation and residual representations (plots of $^{40}\text{Ca} + ^{90}\text{Zr}$ are repeated to show the systematic changes of the three fusions of Ca + Zr), and the excitation function for each system shows a unique oscillatory structure that cannot be reproduced by the multi-Gaussian method. While at the moment not yet explored in this paper, at least 15 more previously mea-

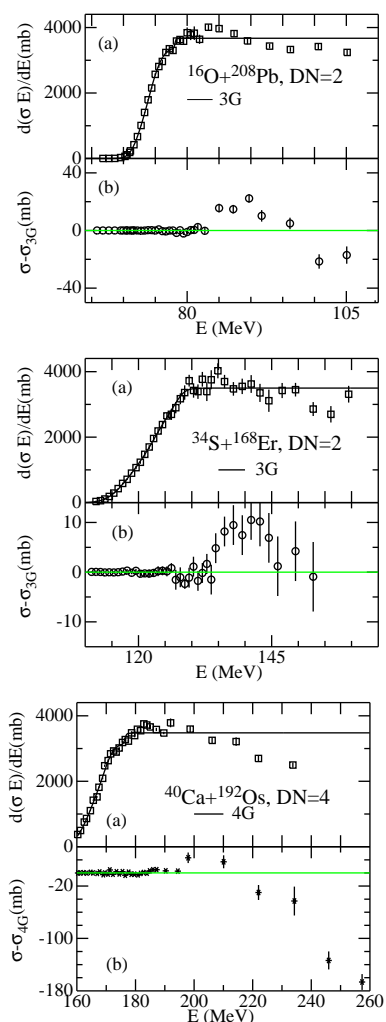


Figure 6. Single-differentiation (a) and residual representation (b) of the fusion excitation function for three different reactions compared to the multi-Gaussian fit method. DN is the step number used in the differentiation process.

sured reactions potentially have the same behavior: $^{40}\text{Ca} + ^{194}\text{Pt}$ [37], $^{40}\text{Ca} + ^{40}\text{Ca}$ [41], $^{40}\text{Ca} + ^{48}\text{Ca}$ [42], $^{48}\text{Ca} + ^{48}\text{Ca}$ [43], $^{58}\text{Ni} + ^{60}\text{Ni}$ [44], $^{58}\text{Ni} + ^{64}\text{Ni}$ [45], $^{32}\text{S} + ^{110}\text{Pd}$ [46], $^{36}\text{S} + ^{110}\text{Pd}$ [46], $^{34}\text{S} + ^{168}\text{Er}$ [38], $^{28}\text{Si} + ^{64}\text{Ni}$ [27], $^{16}\text{O} + ^{144}\text{Sm}$ [35], $^{16}\text{O} + ^{148}\text{Sm}$ [35], $^{17}\text{O} + ^{144}\text{Sm}$ [35], $^{12}\text{C} + ^{92}\text{Zr}$ [47], $^{32}\text{S} + ^{89}\text{Y}$ [48].

This oscillation behavior, although already shown often in experiments, has not been thoroughly explored and explained. While it resembles the behavior described by Poffe and Esbensen for light-mass, symmetric systems, all the systems shown above are in the medium- to heavy-mass regions and are mostly asymmetric. Therefore those arguments cannot be applied. CC calculations seem to reproduce the excitation functions for these reactions well at energies near and below the Coulomb barrier, but not for higher energies.

CC calculations in general were developed for the study of sub-barrier enhancement, where transfer and excitation reaction cross sections dominate the fusion excitation function. Therefore it makes sense these calculations

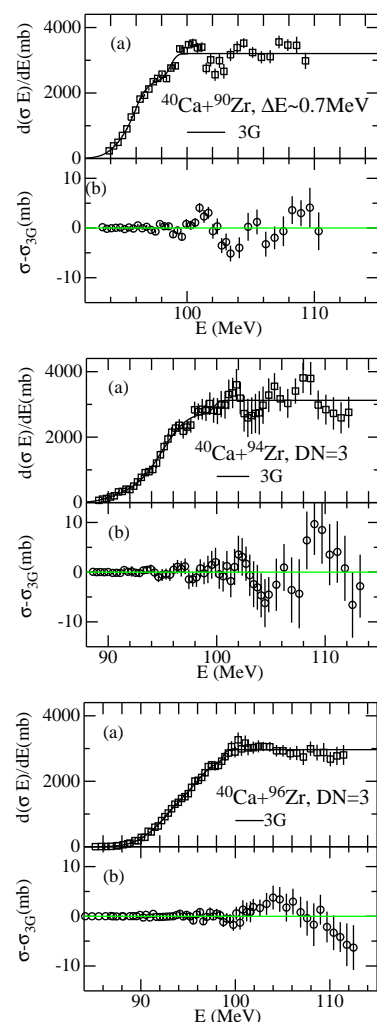


Figure 7. Single-differentiation (a) and residual representation (b) of the fusion excitation function for three different reactions compared to the multi-Gaussian fit method. DN is the step number used in the differentiation process.

reproduce the experimental data well at low energies. In these calculations, the transfer and excitation reactions are treated approximately, and it may be this treatment does not work well at higher energies where channel competition becomes more important than channels coupling. There could also be other factors, including the possibility that the application of the incoming wave boundary condition (IWBC) used in the CC model removes these oscillations. A more complete theoretical model that describes well the fusion excitation function at energies above the barrier is needed to explain this phenomenon.

One step further in the investigation is the combination of the reanalysis tools from both the compound channel observation and the oscillation observation. Mathematically, if the scaled excitation functions for systems forming the same compound nucleus have the same shape, then those same systems should also have the same oscillation phenomenon. Figure 8 shows the first differentiation of the scaled fusion excitation function for systems forming the same compound nucleus ^{216}Ra (a), ^{200}Pb (b),

and ^{170}Hf . While these experiments were performed with much larger energy steps yielding larger uncertainties, the oscillation structures can still be recognized. The results in Figure 8(a-c) show not only overlap in the average values of the excitation function above the barrier, but also in the structures. The dashed blue lines in these plots are to guide the eye for evident "jumps" in the data. Another method to show these overlapping structures is with the scaled residual representation of the fusion cross section, shown in Figure 8(d). Again it appears that both excitation functions exhibit a similar structure with significant overlap, although the uncertainties are large. It may be the oscillation structure is due to the compound channel effect as well.

Considering this phenomenon, further investigation should be taken to explain these structures. Measurements for some of the systems mentioned above should be redone in finer detail, specifically with smaller energy steps and extended to higher energy, so that the structures can be resolved to a better degree. Additionally, an investigation in the experimental gap in the mass range between $^{28}\text{Si} + ^{28}\text{Si}$ and $^{40}\text{Ca} + ^{40}\text{Ca}$, again with small energy steps and a large energy range, will determine if this behavior persists between the light- and medium-mass range.

4 Conclusion

In the reanalysis of previously measured fusion reaction data, two unfamiliar phenomena were observed in fusion excitation functions. The first is a direct influence of the compound nucleus on heavy-ion fusion, where the fusion excitation function shape is unique for reactions that form the same compound nucleus. The second is the observation of oscillatory structure in fusion excitation functions at energies above the barrier that cannot be explained or reproduced by CC calculations. It also appears that these two behaviors are correlated and may be due to the compound channel effect.

Further investigation is suggested, from more experiments with smaller energy steps and to higher energy ranges to more complete theoretical calculations of the excitation function above the barrier that include entrance channel competition and compound channel effects.

This work was supported by the US Department of Energy, office of Nuclear Physics, under Contract No. DE-AC02-06CH11357. The authors want to thank B. B. Back, K. Hagino, G. Montagnoli, K. E. Rehm, and A. M. Stefanini for valuable discussions, and for D. J. Hinde and M. Dasgupta for supplying us their cross-section data file.

References

- [1] M. Dasgupta, D. J. Hinde, N. Rowley, and A. M. Stefanini, *Annu. Rev. Nucl. Part. Sci.* **48**, 401 (1998)
- [2] A. B. Balantekin and N. Takigawa, *Rev. Mod. Phys.* **70**, 77 (1998).
- [3] K. Hagino and N. Takigawa, *Prog. Theor. Phys.* **128**, 1061 (2012).
- [4] B. B. Back, H. Esbensen, C. L. Jiang, and K. E. Rehm, *Rev. Mod. Phys.* **86**, 317 (2014).

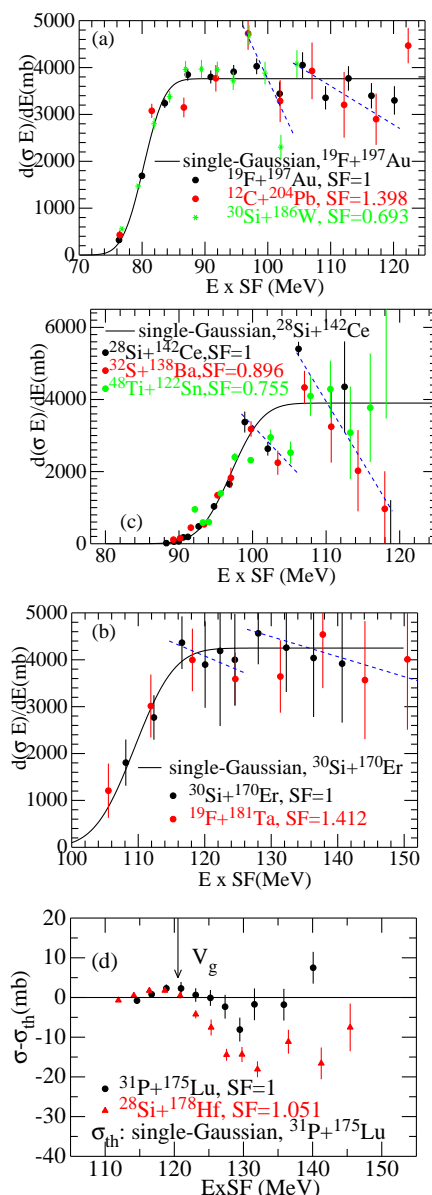


Figure 8. Comparison of the first-differentiation representation of the scaled fusion excitation function for reactions that form the compound nucleus ^{216}Ra (a), ^{200}Pb (b), and ^{170}Hf (c). Dashed lines are to guide the eye. (d) Comparison of the residual representation of the scaled fusion excitation function for reactions that form the compound nucleus ^{206}Rn . All solid lines are the single-Gaussian model fit.

- [5] G. Montagnoli and A. M. Stefanini, *Eur. Phys. J. A* **53**, 169 (2017).
- [6] C. L. Jiang, B. B. Back, K. E. Rehm, K. Hagino, G. Montagnoli, and A. M. Stefanini, *Eur. Phys. J. A* **57**, 235 (2021).
- [7] C. L. Jiang, W. F. Henning, B. P. Kay, and N. Watwood, *Phys. Rev. C* **108**, L051604 (2023).
- [8] C. L. Jiang, W. F. Henning, C. R. Hoffmann, B. P. Kay, and N. Watwood, *Phys. Rev. C* **108**, L051605 (2023).

[9] A. C. Berriman, D. J. Hinde, M. Dasgupta, C. R. Morton, R. D. Butt, and J. Q. Newton, *Nature* **413**, 144 (2001)

[10] D. J. Hinde, A. C. Berriman, R. D. Butt, M. Dasgupta, I. I. Gontchar, C. R. Morton, A. Mukherjee, and J. Q. Newton, *J. Nucl. Radiochem. Sci.* **3**, 31 (2002).

[11] L. F. Canto, D. R. Junior, P. R. S. Gomes, and J. Lubian, *Phys. Rev. C* **92**, 014626 (2015).

[12] P. R. S. Gomes, J. Lubian, I. Padron, and R. M. Anjos, *Phys. Rev. C* **71**, 017601 (2005).

[13] C. L. Jiang, B. B. Back, K. E. Rehm, K. Hagino, G. Montagnoli, and A. M. Stefanini, *Eur. Phys. J. A* **57**, 235 (2021).

[14] C. L. Jiang, K. E. Rehm, B. B. Back, A. M. Stefanini, and G. Montagnoli, *Eur. Phys. J. A* **54**, 218 (2018).

[15] K. Siwek-Wilczynska, E. Siemaszko, and J. Wilczynski, *Acta Phys. Pol. B* **33**, 451 (2002).

[16] K. Siwek-Wilczynska and J. Wilczynski, *Phys. Rev. C* **69**, 024611 (2004)

[17] C. L. Jiang and B. P. Kay, *Phys. Rev. C* **105**, 064601 (2022).

[18] A. Winther, *Nucl. Phys. A* **594**, 203 (1995)

[19] S. Gil, et al., *Phys. Rev. C* **51**, 1336 (1995).

[20] D. J. Hinde, J. R. Leigh, J. O. Newton, W. Galster, and S. Sie, *Nucl. Phys. A* **385**, 109 (1982).

[21] R. D. Butt, D. J. Hinde, M. Dasgupta, A. C. Berriman, A. Mukherjee, C. R. Morton, and J. O. Newton, *Phys. Rev. C* **66**, 044601 (2002).

[22] A. M. Stefanini et al., *Phys. Rev. C* **100**, 044619 (2019).

[23] H. Q. Zhang, C. J. Lin, F. Yang, H. M. Jia, X. X. Xu, Z. D. Wu, F. Jia, and T. Zhang, *Phys. Rev. C* **82**, 054609 (2010).

[24] C. L. Jiang et al., *Phys. Rev. Lett.* **93**, 012701 (2004)

[25] A. M. Stefanini et al., *J. Phys. G: Nucl. Part. Phys.* **48**, 055101 (2021).

[26] D. Ackermann, L. Corradi, D. R. Napoli, C. M. Partrache, A. M. Stefanini, F. Scarlassara, S. Beghini, G. Montagnoli, G. F. Segato, and C. Signorini, *Nucl. Phys.* **574**, 375 (1994).

[27] C. L. Jiang et al., *Phys. Lett. B* **640**, 18 (2006).

[28] A. M. Stefanini et al., *Nucl. Phys. A* **456**, 509 (1986).

[29] E. Almqvist, D. A. Bomley, and J. A. Kucher, *Phys. Rev. Lett.* **4**, 515 (1960).

[30] D. A. Bomley, *Treatise on Heavy-ion Science* (Plenum, New York, 1984), Vol. 3.

[31] N. Poffe, N. Rowley, and R. Lindsay, *Nucl. Phys. A* **410**, 498 (1983).

[32] H. Esbensen, *Phys. Rev. C* **85**, 064611 (2012).

[33] N. Rowley, G. R. Satchler, and P. H. Stelson, *Phys. Lett. B* **254**, 25 (1991).

[34] H. Esbensen and A. M. Stefanini, *Phys. Rev. C* **89**, 044616 (2014)

[35] J. R. Leigh et al., *Phys. Rev. C* **52**, 3151 (1995)

[36] H. Timmers et al., *Phys. Lett. B* **399**, 35 (1997)

[37] M. Dasgupta, D. J. Hinde, A. Diaz-Torres, B. Bouriquet, C. I. Low, G. J. Milburn, and J. O. Newton, *Phys. Rev. Lett.* **99**, 192701 (2007); C. R. Morton, A. C. Berriman, M. Dasgupta, D. J. Hinde, J. O. Newton, K. Hagino, and I. J. Thompson, *Phys. Rev. C* **60**, 044608 (1999).

[38] C. R. Morton, A. C. Berriman, R. D. Butt, M. Dasgupta, A. Godley, D. J. Hinde, and J. O. Newton, *Phys. Rev. C* **62**, 024607 (2000).

[39] J. D. Bierman, P. Chan, J. F. Liang, M. P. Kelly, A. A. Sonzogni, and R. Vandebosch, *Phys. Rev. Lett.* **76**, 1587 (1996); *Phys. Rev. C* **54**, 3068 (1996).

[40] A. M. Stefanini et al., *Phys. Lett. B* **728**, 639 (2014).

[41] M. Montagnoli et al., *Phys. Rev. C* **85**, 024607 (2012)

[42] C. L. Jiang et al., *Phys. Rev. C* **82**, 041601(R) (2010)

[43] A. M. Stefanini et al., *Phys. Lett. B* **679**, 95 (2009)

[44] A. M. Stefanini et al., *Phys. Rev. Lett.* **74**, 864 (1995)

[45] A. M. Stefanini et al., *Phys. Rev. C* **100**, 044619 (2019).

[46] G. M. Zeng et al., *Phys. Rev. C* **57**, 1727 (1998).

[47] J. O. Newton, C. R. Morton, M. Dasgupta, J. R. Leigh, J. C. Mein, D. J. Hinde, H. Timmers, and K. Hagino, *Phys. Rev. C* **64**, 064608 (2001).

[48] A. Mukherjee, M. Dasgupta, D. J. Hinde, K. Hagino, J. R. Leigh, J. C. Mein, C. R. Morton, J. O. Newton, and H. Timmers, *Phys. Rev. C* **66**, 034607 (2002).